JOURNAL OF VIROLOGY, May 2011, p. 4898–4909 Vol. 85, No. 10
0022-538X/11/$12.00 doi:10.1128/JVI.02525-10

A Novel Respiratory Model of Infection with Monkeypox Virus in Cynomolgus Macaques[▽]

Arthur J. Goff,[1]* Jennifer Chapman,[1] Chad Foster,[2] Carly Wlazlowski,[1] Joshua Shamblin,[1] Kenny Lin,[1] Norman Kreiselmeier,[3] Eric Mucker,[1] Jason Paragas,[4] James Lawler,[4] and Lisa Hensley[1]

United States Army Medical Research Institute of Infectious Diseases, Frederick, Maryland[1]; U.S. Army Medical Department Center and School, Fort Sam Houston, Texas[2]; Tripler Army Medical Center, Honolulu, Hawaii[3]; and Integrated Research Facility NIAID/NIH, Frederick, Maryland[4]

Received 3 December 2010/Accepted 28 February 2011

Variola, the causative agent of smallpox, and the related monkeypox virus are both select agents that, if purposefully released, would cause public panic and social disruption. For this reason research continues in the areas of animal model and therapeutic development. Orthopoxviruses show a widely varying degree of host specificity, making development of accurate animal models difficult. In this paper, we demonstrate a novel respiratory infection technique that resulted in "classic" orthopox disease in nonhuman primates and takes the field of research one step closer to a better animal model.

Variola virus (VARV) is a member of the *Poxviridae* family and the etiologic agent of smallpox (SPOX). It causes a devastating disease that is transmitted, most often, via the respiratory route. After seeding the oropharyngeal mucosa, there is a 12- to 14-day incubation period (5). Based on animal modeling and what is known from the human disease, the virus transits the lymph nodes, where it replicates and then enters the bloodstream, producing a primary viremia. This primary dissemination of the virus also targets organs throughout the body, such as the spleen and liver, where it undergoes another replication cycle. Subsequent replication in these organs produces a secondary viremia around days 13 to 15, when the patient develops a fever and malaise, and seeds the next target for replication, the skin. A rash develops as a consequence of viral damage and inflammation, which appears initially on the face and extremities and to a lesser extent over the trunk (i.e., centrifugal distribution).

The rash progresses sequentially from papular to vesicular, to pustular, and ends as scabs and finally desquamating lesions. Most SPOX victims succumb to the disease during the second week of symptoms. Limited pathology records suggest several theories for the cause of death, which include the presence of circulating immune complexes, septic shock, cytopathic effects of the virus, and a cytokine storm (12).

Reported case fatality rates varied from 10 to 30% for classic smallpox and >90% for hemorrhagic forms of the disease. A worldwide vaccination effort eradicated the disease, but the virus still exists in two repositories: the Centers for Disease Control and Prevention (CDC) in Atlanta, GA, and Vector in the Koltsovo region of Russia. The closely related monkeypox virus (MPOX) can also cause disease in humans, with clinical symptoms and disease progression that are indistinguishable from those of SPOX with the exception of MPOX-associated lymphadenopathy. Cessation of worldwide smallpox vaccination has left a large segment of the world population vulnerable to infection with either of these pathogens.

In contrast to variola virus, the presumed broad host range of MPOX precludes eradication, and significant morbidity and mortality are observed in regions of endemicity in Africa (7, 13, 16, 17). The potential for an outbreak of MPOX in the United States was demonstrated in the summer of 2003 when prairie dogs were housed with imported infected Gambian giant pouched rats (*Cricetomys gambianus*), resulting in multiple reported cases of human MPOX (2). The purposeful release of either VARV or MPOX would result in significant morbidity and/or mortality and would likely cause public panic and social disruption. In addition, the underlying mechanisms of SPOX/MPOX virus pathogenesis are only partially understood. For these reasons the continued development of animal models and molecular techniques that will elucidate SPOX and MPOX pathogenesis is necessary.

The development of animal models should take into account (i) the natural route of infection of the virus being modeled, (ii) the natural host, (iii) the likely dose that it would take to produce clinical illness in that host, and (iv) the natural disease course and associated case fatality. To date, the best animal model for SPOX is the intravenous (i.v.) infection of cynomolgus macaques with the Harper strain of VARV. The use of cynomolgus macaques challenged with monkeypox virus (the Zaire '79 strain) has been proposed as a surrogate animal model to limit the experimental use of VARV (6). Although the clinical disease produced in this model is purported to accurately recapitulate VARV and MPOX in humans (from the limited human data available), the intravenous route of infection skips the primary viremia and immediately seeds the internal organs and skin with virus. In addition, the intravenous route of infection is artificial, as transmission of MPOX and SPOX is believed to be through close contact or droplet for-

* Corresponding author. Mailing address: United States Army Medical Research Institute of Infectious Diseases, 1425 Porter St., Virology Division, Viral Therapeutics Branch, 903Q, Fort Detrick, MD 21702-5011. Phone: (301) 619-4836. Fax: (301) 619-8552. E-mail: Arthur.Goff@amedd.army.mil.

▽ Published ahead of print on 9 March 2011.

mation and the dose required to experimentally produce severe clinical disease is quite high (5×10^7 PFU).

As mentioned, both VARV and MPOX are transmitted by close contact and/or the respiratory route. Early attempts at producing a disease that resembles classic, ordinary smallpox by respiratory infection were met with variable results. While exposure of cynomolgus monkeys to MPOX in a head-only exposure chamber using a 3-jet collison nebulizer inside a class III biological safety cabinet under the control of an automated bioaerosol exposure system succeeded in producing significant disease, attempts at using a similar system for VARV failed (18). In addition, the use of the head-only exposure chamber with a collison nebulizer has been criticized because the actual inhaled dose for each monkey varies, making meaningful statistical analyses difficult, and the quantity of virus required for these experiments is quite large. Work in our laboratory demonstrated that exposure of nonhuman primates by the intratracheal (i.t.) route using a 1- to 5-ml bolus of liquid inoculum of MPOX produced consistent results; however, the resulting pathology appeared inconsistent with human SPOX disease because the bolus inoculum produced a lobar pneumonia (unpublished data). In pilot studies at the CDC, intratracheal administration of 1×10^8 VARV produced a lethal disease in 1/3 of the nonhuman primates. This is consistent with the mortality rate of intravenous challenges with this dose of virus and with the mortality rate of SPOX in humans. While the intratracheal bolus did not allow us to lower the dose of the virus needed to cause disease, it did demonstrate that nonhuman primates (NHPs) were susceptible to challenge with VARV by routes other than intravenous methods and supported the idea that alternatives to classic aerosol exposure methods needed to be developed.

In this paper, we describe the development of a novel challenge technique using a microsprayer attached to a bronchoscope, along with a high-pressure syringe for infecting cynomolgus macaques with MPOX virus by delivering an aerosol directly above the tracheal carina. While the particle size (~8 μm) is larger than that typically generated by collison nebulizers (~1 to 3 μm), this method consistently (i) allowed for a dose-dependent incubation period before onset of clinical disease, (ii) allowed for development of a disease that resembles classic, ordinary smallpox disease with systemic dissemination, and (iii) resulted in pathology that is consistent with inhalation of monkeypox virus. In addition, the amount of virus required to produce significant disease was lowered by at least a log compared to the intravenous infection model. The model system presented in this paper provides an alternative for the assessment of risks from aerosol exposures to orthopoxviruses as well as a mechanism for the evaluation of candidate vaccines and therapeutics for preventing or treating disease that occurs as the direct result of aerosol exposures. This model will be critical to the ultimate goal of fulfilling the FDA requirements outlined in the Animal Rule: to have a well-characterized animal model for vaccine and chemotherapeutic testing when human efficacy studies are not ethical or feasible (4). In addition, the data presented here, as well as pilot studies performed with intratracheal bolus administration of VARV, suggest that this may be an alternative solution for exposure of NHPs to this virus by routes other than the intravenous approach.

MATERIALS AND METHODS

Virus preparation and cells. Monkeypox virus strain Zaire was propagated from scab material on chorioallantoic membranes, and one passage in LLC-MK2 cells, two passages in BSC-40 cells, and two passages in Vero cells followed. The virus stock was quantified via plaque assay on Vero E6 cells, as was the diluted inoculum after challenge.

Nonhuman primates and infection. Orthopox-negative cynomolgus macaques were challenged with MPOX using a bronchoscope in conjunction with a liquid MicroSprayer aerosolizer, model IA-1C, and an FMJ-250 high-pressure syringe (Penn-Century, Inc.) to deliver a large particle aerosol directly above the tracheal carina. Phlebotomy, lesion counts, and physicals were performed. Longitudinal blood samples were collected for hematology, chemistry, and detection viral sequences.

Hematology. Total white blood cell (WBC) counts, white blood cell differentials, red blood cell counts, platelet counts, hematocrit values, total hemoglobin, mean cell volume, mean corpuscular volume, and mean corpuscular hemoglobin concentration were determined from blood samples collected in tubes containing EDTA, using a laser-based hematologic analyzer (Coulter Electronics, Hialeah, FL).

Chemistry. Concentrations of albumin (ALB), amylase (AMY), alanine aminotransferase (ALT), aspartate aminotransferase (AST), alkaline phosphatase (ALP), gamma-glutamyltransferase (GGT), glucose (GLU), cholesterol (CHOL), total protein (TP), total bilirubin (TBIL), urea nitrogen (BUN), chloride (Cl^-), potassium (K^+), and creatinine (Cr) were measured using a Piccolo point-of-care blood analyzer (Abaxis, Sunnyvale, CA).

Detection of viral load. To evaluate viral load, DNA extractions were performed on whole blood using a Qiagen QiAMP DNA blood minikit (Valencia, CA), and quantitative PCR was performed as previously described (10). Complete necropsies were performed, and tissues were collected for pathology and virus quantification.

Necropsy. A necropsy was performed on all animals, either as soon as death occurred from infection or after humane euthanasia of terminally ill or moribund animals. Animals that survived infection were euthanized 21 to 25 days postinfection. All tissues were immersion fixed in 10% neutral buffered formalin.

Histology and immunohistochemistry. Formalin-fixed tissues for histologic examination were trimmed, processed, and embedded in paraffin according to established protocols (15). Histology sections were cut at 5 μm, mounted on glass slides, and stained with hematoxylin and eosin (H&E). Phosphotungstic acid-hematoxylin (PTAH)-stained sections of the kidney were evaluated to confirm the presence of polymerized fibrin. Immunohistochemical staining was performed on replicate tissue sections using an Envision+ kit (Dako, Carpinteria, CA). Briefly, sections were deparaffinized in Xyless and rehydrated in graded ethanol, and endogenous peroxidase activity was quenched in a 0.3% hydrogen peroxide-methanol solution for 30 min at room temperature. Slides were washed in phosphate-buffered saline (PBS), and then sections were incubated in the primary antibody, a rabbit polyclonal antibody against vaccinia virus (USAMCIID no. 1293), diluted 1:3,500 for 60 min at room temperature. Sections were washed in PBS and incubated for 30 min with Envision+ rabbit secondary reagent (horseradish peroxidase-labeled polymer) at room temperature. Peroxidase activity was developed with 3,3′-diaminobenzidine (DAB), counterstained with hematoxylin, dehydrated, cleared with Xyless, and then coverslipped.

Lab animal usage. All research was conducted in compliance with the Animal Welfare Act and other federal statutes and regulations relating to animals and experiments involving animals and adheres to principles stated in the *Guide for the Care and Use of Laboratory Animals* (14). The facility where this research was conducted is fully accredited by the Association for Assessment and Accreditation of Laboratory Animal Care International.

RESULTS

Initial studies of intratracheal administration of virus were performed using a 1- to 5-ml bolus administration of MPOX (~5×10^7 PFU), resulting in a rapidly fatal disease course with marked lobar pneumonia. Pilot studies using bolus administration of the VARV (~1×10^8) Harper strain also produced significant disease, with 1/3 of the animals succumbing. In dose-seeking experiments using the bronchoscope/microsprayer, groups of three animals each were infected in a stepwise fashion with 3.42×10^6, 8.37×10^6, or 3.53×10^7 PFU of

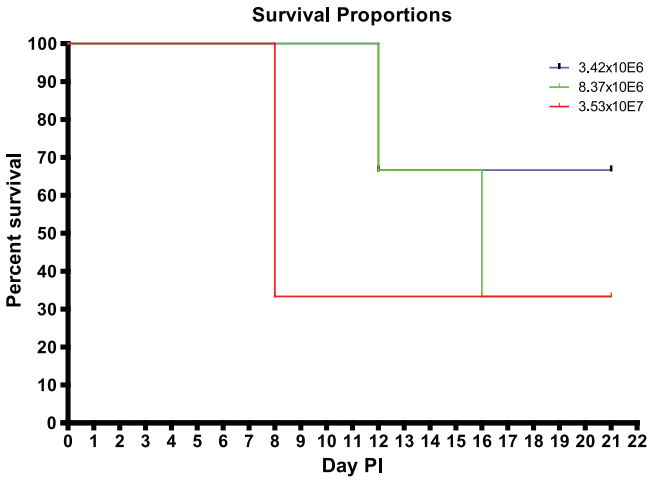

FIG. 1. Survival curve for intratracheal instillation of monkeypox virus. Groups of three animals each were infected in a stepwise fashion with 3.42×10^6, 8.37×10^6, or 3.53×10^7 PFU of monkeypox Zaire '79.

MPOX Zaire '79. At the lowest dose, one animal succumbed to MPOX disease on postinfection day (PID) 12 (Fig. 1). The middle dose resulted in two deaths attributable to monkeypox on PIDs 12 and 16. This highest dose resulted in two deaths, both on PID 8.

Clinical disease group with dose of 3.42×10^6 PFU. Animals in the low-dose group (3.42×10^6 PFU) developed a fever beginning on PID 4. Two of the three animals returned to normal temperatures by PID 8. The temperature of the third animal remained elevated until it succumbed on PID 12. Decreases in weight were detected in all three animals as early as PID 4. Animals 2 and 3 sustained a total of a 10% weight loss before they began to recover, while animal number 1 was approximately 15% below the starting weight on the day of death. All three animals in this dose group displayed similar hematological changes (Fig. 2), with the exception of the white blood cell counts. Monkey no. 1 showed an 8-fold increase over the baseline value, while the other two animals (monkey no. 2 and monkey no. 3) showed only an approximate 2-fold increase. Blood chemistry values for all three animals did change over the course of infection, but with no identifiable trend except for blood urea nitrogen levels (Fig. 3). The BUN value for monkey no. 1 almost doubled in the 24 h prior to death.

Lymphadenopathy became evident between PIDs 6 and 8. Pox lesions were first observed during clinical examination on PID 8 in the following locations: oral cavity, head, arms, chest, abdomen, groin, legs, and tail. Lesions were more concentrated in the oral cavity, and in the axillary and inguinal regions. The lesions progressed sequentially from a papular rash to a vesicular rash to a pustular rash and ended as scabs and desquamating lesions. Total lesion numbers on the first day of appearance ranged from 64 to 131 on each animal and reached a maximum of between 216 and 304 (Fig. 4). In the two survivors, lesions began scabbing between PIDs 12 and 14 and desquamating between PIDs 16 and 18. Viral DNA was quantifiable in the blood beginning on PID 4 (Fig. 4). Viral DNA in whole blood increased steadily until about PID 12. Peak titers were close to 5.0×10^6 genomes/ml in two out of three animals and 5.0×10^5 genomes/ml in the third. Viral DNA in the blood of all three animals typically did not vary by more than a log through the course of infection. Viral genomes were below the limit of quantification in the two survivors by PID 16.

Clinical disease group with dose of 8.37×10^6 PFU. Animals in the middle dose group (8.37×10^6 PFU) displayed clinical features similar to those of the low-dose group. While two of the three animals died from acute MPOX disease, the third animal died at PID 22. There were no outward clinical signs of illness in this animal other than desquamating MPOX lesions; however, postmortem examination and histology revealed evidence of a secondary bacterial infection. All three animals developed fever around PID 4. The temperatures for monkey no. 4 and monkey no. 5 remained elevated until they succumbed on PIDs 12 and 16, respectively. The temperature of monkey no. 6 began to return to baseline after PID 10 but spiked again on PID 20. All three animals in this dose group sustained greater than a 10% weight loss. Approximately a 2-fold increase in the WBCs was observed in monkey no. 4 and monkey no. 5 on PID 10 (Fig. 2). WBCs peaked at PID 10 in these animals. Two distinct increases in WBCs were observed with monkey no. 6, with a 1.5-fold increase on PID 10 and a 2-fold increase PID 20. Platelet counts were close to 2-fold higher on the day of death in monkeys no. 5 and 6, but platelet counts barely increased at all in monkey no. 4. Just as in the previous dose group, the BUN levels increased sharply in all three animals the day before death.

Lymphadenopathy was also observed in all three animals beginning around PID 6 and 8. Lesions appeared on PID 6 (Fig. 4) in two out of three animals and followed an appearance and distribution pattern similar to those of the low-dose group. Lesion counts in monkey no. 4 climbed sharply between PIDs 6 and 10 and peaked at 552 lesions. Monkey no. 5 peaked at 466 lesions, and monkey no. 6 at 315 lesions. Viral genomes in the blood increased through PID 10 and peaked in the 10^7 range.

Clinical disease group with dose of 3.53×10^7 PFU. The three animals in the high-dose group (3.53×10^7 PFU) followed a similar, although accelerated disease course, with two succumbing on PID 8 and with some animal-to-animal variations noted. Fever developed in two animals on PID 4 and on PID 6 in the third animal. Temperature remained elevated for less than 48 h in all three animals. In the one animal that survived, the body temperature returned to baseline, while the core body temperature of the two animals that succumbed dropped below baseline at the terminal stages. All three animals began to lose weight and sustained close to a 10% weight loss during the course of the study. Animal no. 7 survived infection (resolving lesions and clearing viral genomes to below the limit of quantification) and was euthanized on PID 21 due to the complete recovery from monkeypox disease. The WBC count in monkey no. 8 increased almost 6-fold over the baseline, while the counts in the other two animals showed only a minimal increase (Fig. 2). Red blood cell counts and platelet counts for all three animals underwent comparable moderate increases compared to baseline values. Blood urea nitrogen levels in monkey no. 8 increased 4-fold before death but barely increased at all in monkey no. 9. All other blood chemistry analytes were comparable.

Lymphadenopathy was first observed on PID 6 and lesions

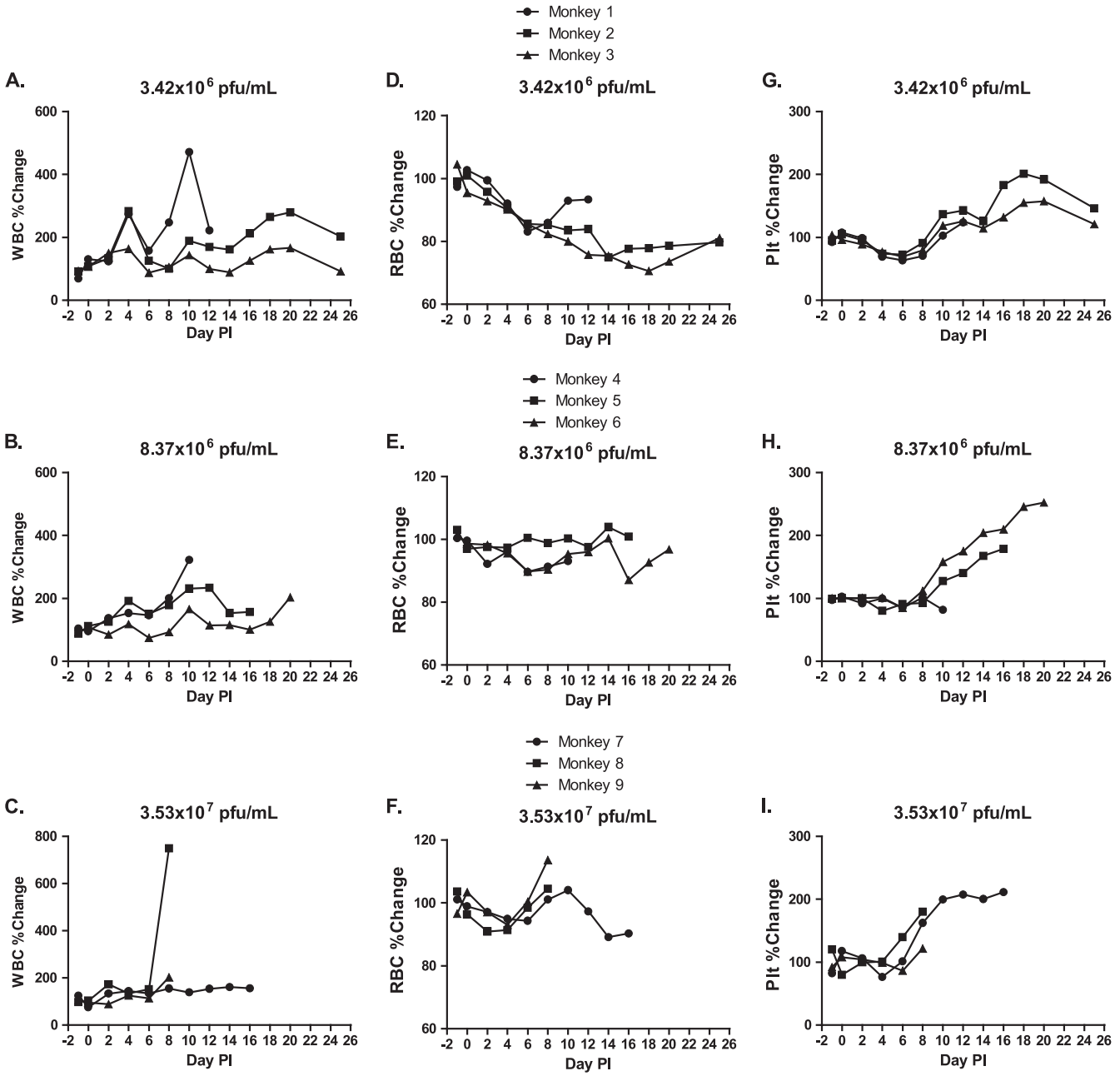

FIG. 2. Hematology for NHPs infected with the microsprayer. Changes in WBC counts in low, medium, and high doses (A to C); RBC counts (D to F); and % platelets (Plt) (G to I) are depicted.

first appeared on PID 4 in two out of three animals (Fig. 2) in this group. Lesion counts for monkey no. 8 reached 350, while lesion counts for monkeys no. 7 and 9 reached only 85 and 22, respectively. Viral genomes in the blood of monkey no. 8 approached 10^9 genomes/ml, while genome levels in monkeys no. 7 and no. 9 reached only 10^5 genomes/ml. Viral genomes in the blood were below the limit of quantification in the survivor by PID 14.

Necropsy findings. (i) Gross. Postmortem examination was performed on all animals. Animals that succumbed or were euthanized at the terminal stage of disease had similar gross pathological findings, regardless of dosage group. Fibrinonecrotic bronchopneumonia was a consistent finding; the lungs were edematous and red and failed to collapse (Fig. 5C, 6C, and 7A). There were often multiple necrotic foci (Fig. 5C) and occasional fibrinous pleural adhesions (Fig. 7A). The trachea contained bloody froth and had multifocal or coalescing necrotic, dark-red mucosal lesions, often more severe near the carina where instillation of the virus occurred. Other gross lesions observed included vesiculopustular, umbilicated, and scabbed cutaneous lesions (Fig. 5A and 6A), oral ulcers (Fig. 5B), enlarged peripheral lymph nodes, and proliferative and necrotizing or ulcerative lesions in the esophagus, stomach, and urinary bladder. In addition, several animals displayed

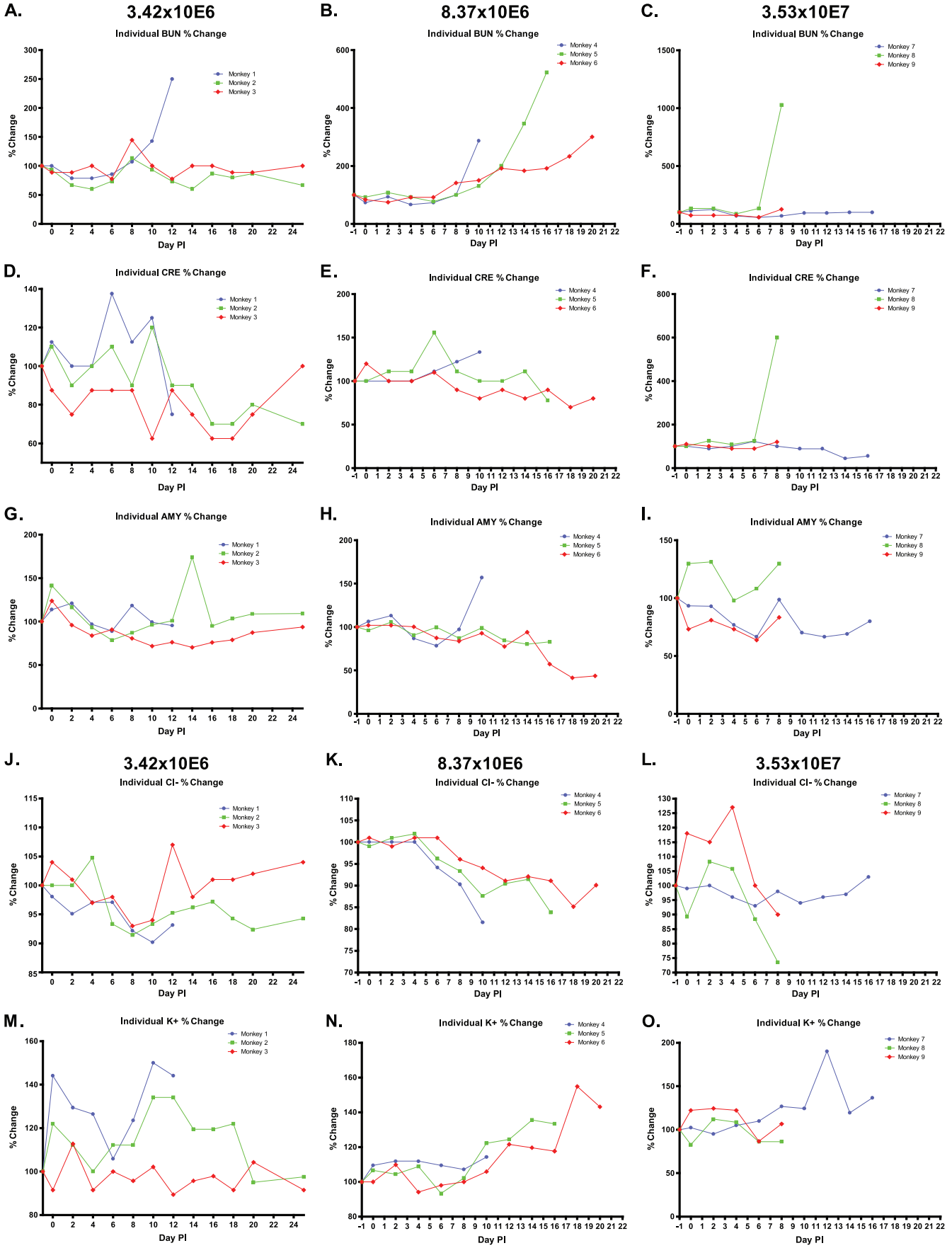

FIG. 3. Blood chemistries for NHPs infected with the microsprayer. Changes in BUN counts in low, medium, and high doses (A to C); CRE (D to F); AMY (G to I); Cl- (J to L); and K+ (M to O) are depicted.

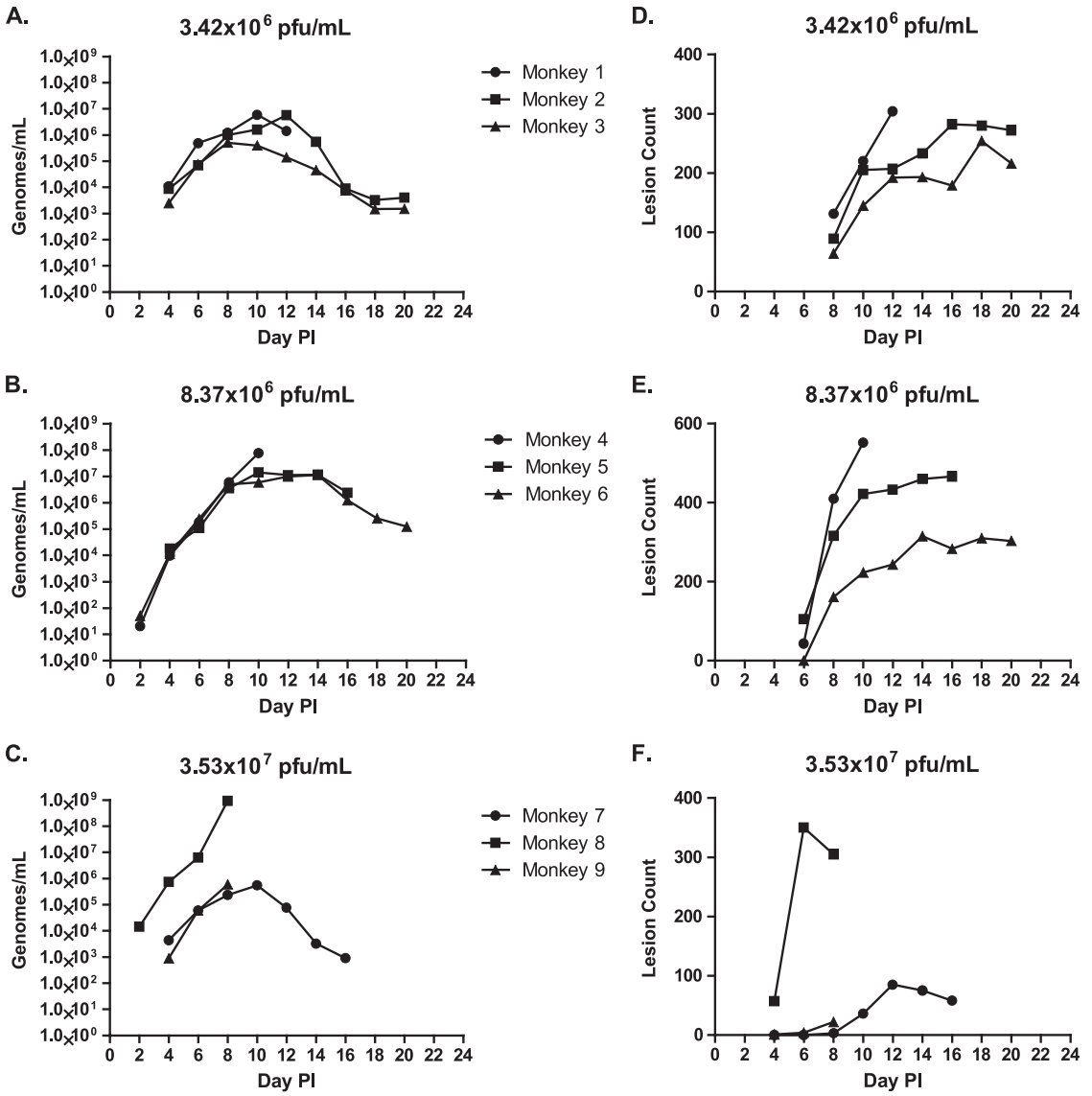

FIG. 4. Viral load (genomes/milliliter of whole blood) and lesion counts for NHPs infected with the microsprayer. Genome levels in whole blood in low, medium, and high doses (A to C) and lesion counts (D to F) are shown.

evidence of hemorrhagic disease (monkey no. 8, high dose, and monkeys no. 4 and 5, middle dose) to include a petechial rash, subpleural hemorrhage (Fig. 8A), and testicular hemorrhage. One of these animals (monkey no. 5) died on PID 16 and had evidence of peritonitis, which is an unusual lesion in monkeypox virus-infected NHPs.

Animals that survived infection and were euthanized at the end of the study had discrete areas of necrosis in the lung, pulmonary fibrosis and edema, fibrous pleural adhesions, and tracheal congestion. Other gross lesions included scabs and desquamated skin lesions, enlarged peripheral and tracheobronchial lymph nodes, and splenic lymphoid hyperplasia.

In the animal that had the secondary bacterial infection (monkey no. 6), gross lesions included diffuse fat and muscle atrophy, scabbed cutaneous lesions, gingival ulcers, enlarged peripheral lymph nodes, pleural adhesions, bronchointerstitial pneumonia and pulmonary edema, laryngeal inflammation and edema, mediastinal inflammation and edema, discrete areas of necrosis in the splenic capsule, pericarditis, and pericardial effusion.

(ii) Histology. Key histopathologic lesions are outlined in Table 1 and were not dose dependent. In animals that succumbed or were euthanized due to advanced disease, lesions consisted of fibrinonecrotic bronchopneumonia (Fig. 5D, 7B, and 8B), necrosis of the trachea and surrounding mediastinal tissues, pulmonary edema, and pleuritis. Other lesions included necrosis in multiple tissues, including the skin (Fig. 6B), tonsils, tongue, lip, larynx, pharynx, esophagus, stomach, small and large intestines, liver, epididymis, testes, prostate gland, pituitary gland, adrenal gland, conjunctiva, urinary bladder, lymph nodes, thymus, spleen, bone marrow, skeletal muscle, sciatic nerve, and brachial plexus; lymphoid depletion in multiple lymphoid tissues; and hepatocellular eosinophilic intracytoplasmic inclusion bodies.

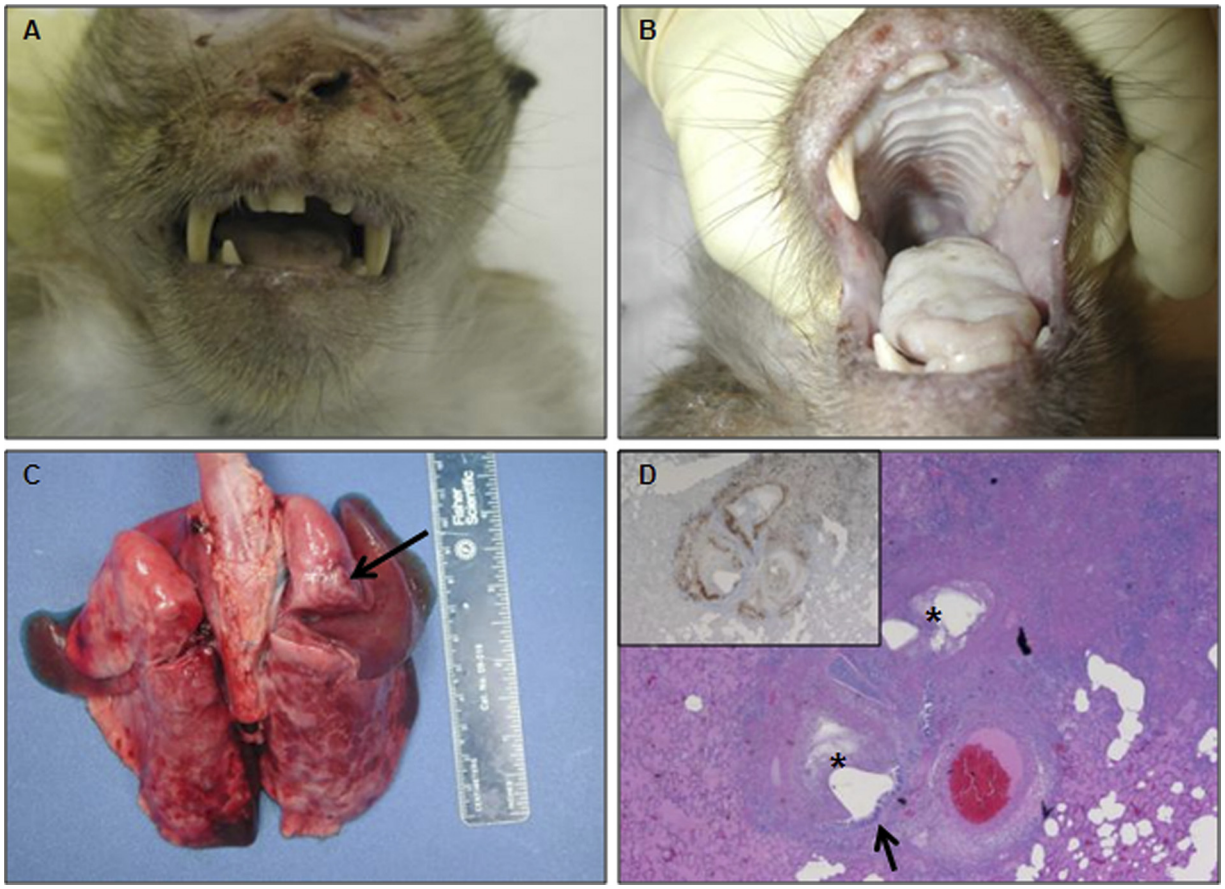

FIG. 5. Lesions associated with intratracheal monkeypox virus infection in animal 1 (low-dose group) on day 12 postinfection. (A) Facial exanthema. Vesicopustular lesions on the bridge of the nose and ulcerative lesions on the lips. (B) Ulcerative stomatitis. Note the proliferative rim surrounding ulcers, a prominent feature typical of orthopoxvirus lesions associated with mucous membranes. (C) Necrotizing bronchopneumonia and pleuritis. The lungs are diffusely noncollapsing and multifocally mottled red with consolidation of the right middle lobe and caudal segment of the left cranial lobe. There are multifocal raised tan lesions (necrosis, arrow). (D) Lung, fibrinonecrotic bronchopneumonia. Inflammation and necrosis are centered on bronchi and bronchioles and extend into the adjacent interstitium, obscuring pulmonary architecture. Bronchial epithelium is degenerate to necrotic and sloughed into the lumen, where it is admixed with fibrin and edema (asterisks). Multifocally, the bronchial epithelium is hyperplastic (arrow). Alveoli are multifocally filled with edema and fibrin. H&E. Inset: replicate section demonstrating immunoreactive epithelial cells lining bronchi, as well as intracellular and extracellular viral antigen in areas of necrosis. Immunoperoxidase method using rabbit polyclonal antibody to vaccinia virus; hematoxylin counterstain.

In addition to the lesions typical of monkeypox virus infection, several animals (monkeys no. 4, 5, and 8) displayed evidence of disseminated intravascular coagulation (DIC), including intravascular fibrin thrombi (Fig. 8D) and hemorrhage in multiple organs (Fig. 8C). These animals were either in the middle- or high-dose challenge groups.

Animals that survived and were euthanized at the end of the study had discrete areas of pulmonary and splenic necrosis and inflammation, alveolitis and bronchitis, and necrotizing sciatic neuritis. Scabbed and desquamated skin lesions collected for histological examination revealed only superficial perivascular dermatitis, but no corresponding immunoreactivity was present in these lesions. Other microscopic lesions interpreted to be related to monkeypox virus infection included lymphoid hyperplasia, plasmacytosis, and subacute to chronic tracheitis.

In addition to the typical lesions caused by monkeypox infection, additional histologic lesions present in the animal with the bacterial coinfection included the following: neutrophilic and histiocytic inflammation in the larynx, pharynx, mediastinum, tonsil, lungs, kidneys, colon, spleen, bone marrow, and skin; discrete areas of necrosis and inflammation in the colonic serosa and splenic capsule; necrotizing perivasculitis; fibrinoid vasculitis; intravascular fibrin thrombi; and intrahistiocytic and extracellular bacteria. Since bacterial infection was not suspected at necropsy, culture of tissues was not performed; however, Gram stains identified Gram-negative rods, and PCR further identified *Klebsiella pneumoniae* as the cause of this secondary infection.

(iii) Immunohistochemistry. Immunohistochemical evaluation of tissues in animals that succumbed or were humanely euthanized due to advanced disease confirmed that the pathological changes were due to intratracheal inoculation with monkeypox virus, followed by systemic dissemination. Similar to gross and histologic findings, differences in immunohistochemical staining patterns were observed only between survivors and nonsurvivors. No differences were observed among the three dosage groups. Immunoreactivity involved the following: mononuclear inflammatory cells in tissue and in

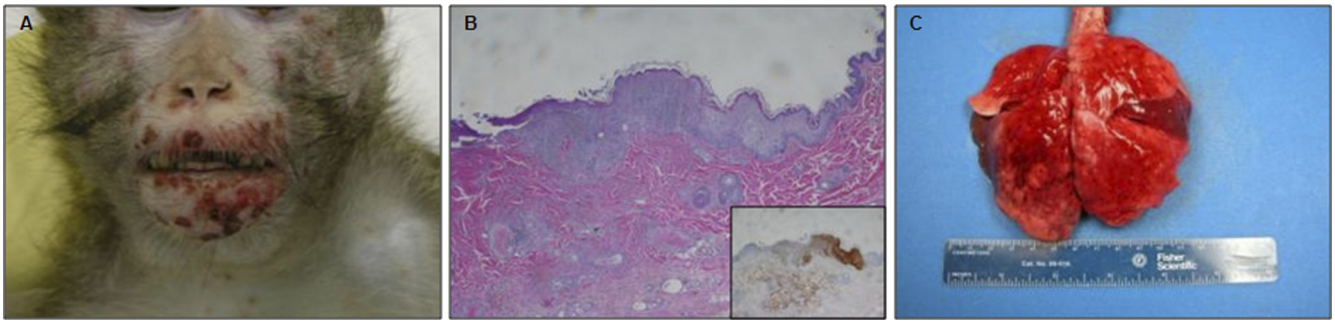

FIG. 6. Lesions associated with intratracheal monkeypox virus infection in animal 5 (medium-dose group) on day 16 postinfection. (A) Exanthema. Pustules and scabs present on the face and neck. Note umbilication of lesions, most prominent around the nares. (B) Haired skin, necrotizing and proliferative dermatitis. The epidermis is hyperplastic with ballooning degeneration and necrosis. In the underlying dermis, collagen bundles are surrounded and separated by inflammatory cells and necrotic debris. H&E. Inset: replicate section demonstrating intracellular viral antigen in affected epithelium and scattered inflammatory cells and fibroblasts in the dermis. Immunoperoxidase method using rabbit polyclonal antibody to vaccinia virus; hematoxylin counterstain. (C) Necrotizing bronchopneumonia and pleuritis. The lungs are diffusely red, failed to collapse, and have multifocal raised pale pleural lesions.

circulation; areas of necrosis in various tissues (Fig. 5D, inset); and hyperplastic, degenerate, and necrotic epithelial cells in the skin (Fig. 6B, inset) and mucosa of affected tissues. In areas of necrosis, there was often extracellular viral antigen associated with the cellular debris. Hepatocytes were immunoreactive in two animals that succumbed to disease (monkeys no. 4 and 8 [both of these animals had hemorrhagic manifestations]). In these same two animals, circulating mononuclear cells, endothelial cells, and spindle cells in connective tissues were immunoreactive, so there was at least minimal immunopositivity in every tissue examined. The animal euthanized on PID 16 (monkey no. 5) had positive immunoreactivity in lesions, similar to animals that succumbed at earlier times postchallenge, as well as immunoreactivity in the serosa of the urinary bladder, testes, epididymis, duodenum, jejunum, ileum, cecum, and colon, all likely as a result of the peritonitis. The *Klebsiella*-infected animal that died on day 22 postinfection (monkey 6) had positive immunoreactivity in areas of necrosis and inflammation (similar to animals that succumbed) and also in the necrotic centers of discrete areas of splenic and colonic necrosis (similar to animals that survived infection with MPOX).

Some tissues with no histomorphologic changes had positive immunoreactivity and included the following: the mediastinal and axillary perinodal adipose tissue, cells in the seminiferous tubules, and cells in the lamina propria of the colon (monkey 1); the tongue, submandibular salivary gland, nose, kidney, and duodenum (monkey 8); and epithelial cells lining Rathke's pouch in the pituitary gland, adrenocortical cells, and cells in the stomach, pancreas, cecum, and colon (monkey 4). Two of these three animals with immunoreactivity in tissues without morphological alterations had hemorrhagic manifestations of the disease.

DISCUSSION

Currently, one of the most well-characterized models of MPOX in nonhuman primates is an intravenous infection

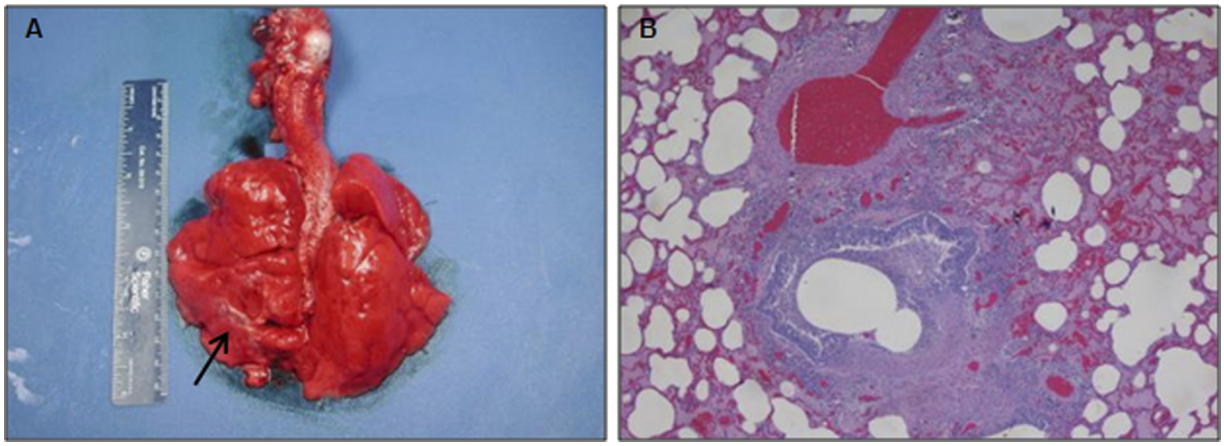

FIG. 7. Lesions associated with intratracheal monkeypox virus infection in animal 9 (high-dose group) on day 8 postinfection. (A) Necrotizing bronchopneumonia and pleuritis. Lungs are diffusely red, heavy, and wet. There are fibrinous adhesions on the pleural surface that were attached to the thoracic wall and diaphragm (arrow). (B) Lung, fibrinonecrotic bronchopneumonia. In a focally extensive area, necrotic debris, degenerate inflammatory cells, and fibrin efface bronchial epithelium and extend into the adjacent interstitium. Also note the hyperplastic epithelium lining the bronchus. H&E.

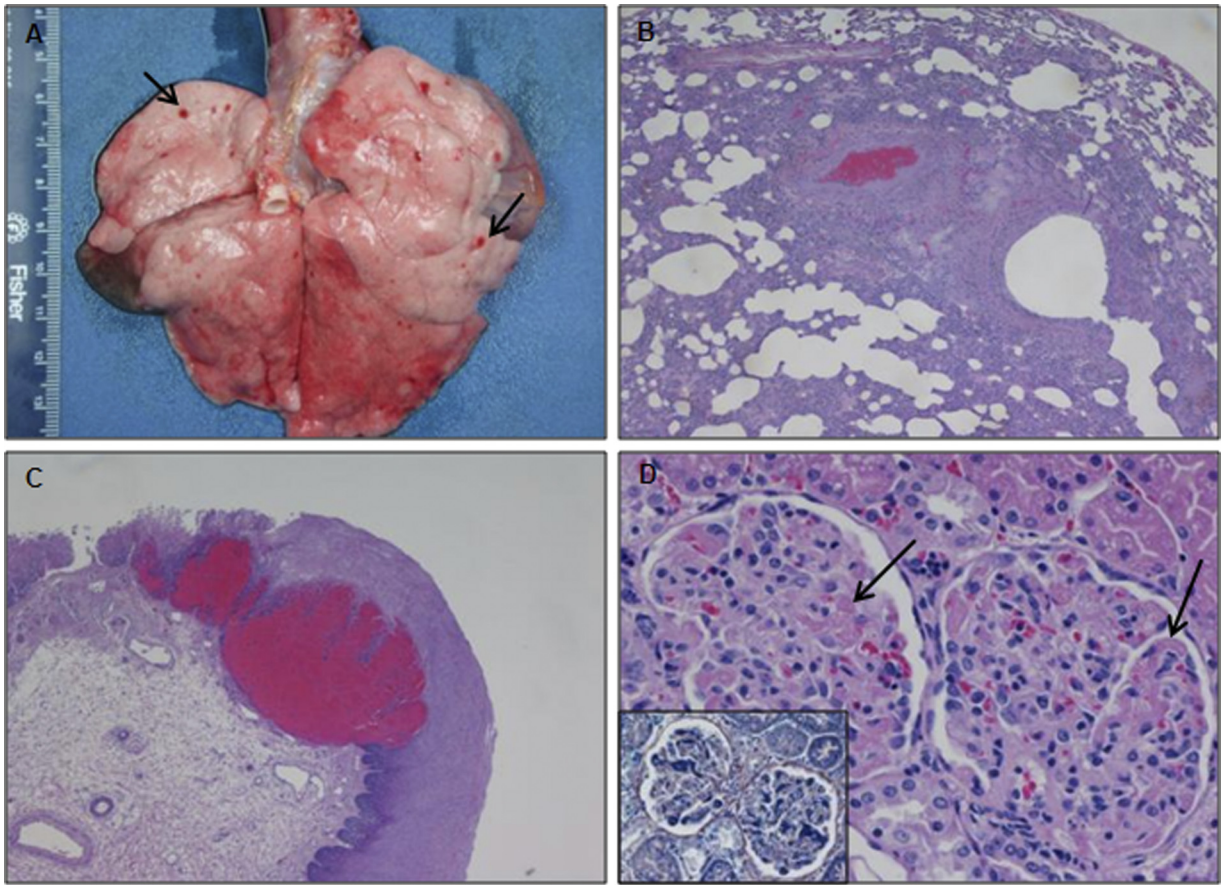

FIG. 8. Hemorrhagic lesions associated with intratracheal monkeypox virus infection. Animal 8 (high-dose group) on day 8 postinfection (A to C); animal 4 (medium-dose group) on day 12 postinfection, kidney (D). (A) Necrotizing bronchopneumonia with subpleural hemorrhages (arrows). (B) With the exception of subpleural hemorrhage (not shown in this image), the histologic appearance of the lungs in this animal is comparable to animals without hemorrhagic manifestation of disease: epithelial necrosis and inflammation in large airways and similarly affected interstitium (compare to 5D and 7B). H&E. (C) Necrohemorrhagic and proliferative esophagitis. Note coalescing areas of hemorrhage at the mucosal-submucosal junction and confined to the mucosa by a thin rim of basilar epithelial cells. There is also marked submucosal edema. H&E. (D) Intravascular fibrin thrombi are present within glomerular vessels (arrows). H&E. Inset: fibrin (blue fibrillar material) is present within glomerular vessels. PTAH.

model. While useful, this route of infection bypasses the incubation and primary viremia stages of disease and creates a high artificial secondary viremia. From the point of secondary viremia, the model recapitulates human MPOX/SPOX reasonably well (6, 9). However, the fact that the infection route is not respiratory and that there is no incubation phase complicates attempts to use this model for screening candidate therapeutics and vaccines, particularly for those that will be labeled for use for protection from aerosol exposures. The steep dose response curve for the challenge dose further limits the usefulness of this model for detecting minor to moderate changes in the virulence and pathogenesis of different strains of virus.

The aerosol exposure model has been suggested as an alternative to the intravenous model (18). Original attempts in developing aerosol models for orthopoxviruses utilized a head-only aerosol chamber with a three-jet collison nebulizer to deliver a small-particle aerosol. While this method did produce significant disease, it required large quantities of virus, and the delivered dose was unpredictable. Additionally, previous attempts at VARV aerosol challenges failed either due to the lack of specialized facilities for aerosolization or an inadequate amount of virus required for challenge. Although the original aerosol models did allow for an incubation phase and primary viremia, the minimal numbers of lesions often observed with aerosolization of the virus led some to question the faithfulness of this model. In addition, generation of the aerosol requires expensive facilities and equipment as well as specialized staff. We set out to develop, as an alternative to the traditional aerosol and intravenous models, a method/model for delivery of virus that would simulate a potential biological weapons exposure.

In early experiments, a bronchoscope was used to deliver a 1- to 5-ml bolus of liquid inoculum of MPOX or VARV into the trachea of cynomolgus macaques (unpublished data). This methodology resulted in death of the animals from a severe lobar bronchopneumonia (data not shown), a distribution that has not commonly been associated with human infection with MPOX or VARV. In addition, animals infected by using the bolus of virus delivered intratracheally often succumbed to respiratory stress before any classical clinical signs of MPOX

TABLE 1. Key histopathologic lesion scores

Location or type of lesion	Histopathologic score of indicated animal no.[a]								
	1	2	3	4	5	6	7	8	9
Haired skin									
Epidermal degeneration/necrosis and ballooning degeneration	3	−	−	4	3–4	3–4	−	3–4	−
Epidermal hyperplasia	3	2	1	4	3–4	3–4	2	3–4	−
Hemorrhage	−	−	−	+	−	−	−	−	−
Subacute to chronic inflammation	−	2	1	−	−	−	2	−	−
Lip and Nares									
Epithelial degeneration/necrosis	4	−	−	2–4	2–5	3–4	N/A	−	3
Epithelial hyperplasia	4	3	1	−	2–5	3–4	N/A	1	2–3
Perivascular inflammation only	−	1	1	−	−	−	N/A	1	−
Inguinal and axillary lymph nodes									
Lymphoid depletion	1	−	−	3–4	−	−	−	3–5	−
Necrosis	1	−	−	3–4	−	−	−	3–5	1–2
Hemorrhage	−	−	−	−	−	−	−	+	−
Lymphoid hyperplasia	−	1	2	−	2	1–2	−	−	−
Plasmacytosis	−	2–3	−	−	2–3	1–2	−	−	−
Testis									
Necrosis	1–3	−	−	3	4	−	−	2	−
Hemorrhage	−	−	−	+	+	−	−	−	−
Liver									
Degeneration/necrosis	−	−	−	3	−	−	−	3–4	−
Intracytoplasmic inclusion bodies	−	−	−	+	−	−	−	+	−
Spleen									
Lymphoid depletion	3	−	−	4	−	3	−	4–5	3–4
Necrosis	2	−	−	4	−	−	−	4–5	3–4
Lymphoid hyperplasia	−	−	2	−	−	−	3	−	−
Nodular areas of necrosis/inflammation	−	−	−	−	−	3	3	−	−
Lung									
Fibrinonecrotic pneumonia	5	−	−	4–5	4	3–4	−	3–4	4
Pleuritis	5	−	4–5	4–5	4	−	4	−	4
Hemorrhage	−	−	−	+	−	−	−	+	−
Nodular necrosis/inflammation and fibrosis	−	4–5	4–5	−	−	−	4	−	−
Mediastinal lymph node									
Lymphoid depletion	−	−	−	4	−	2	−	5	−
Necrosis	−	−	−	4	4	−	−	5	3
Hemorrhage	−	−	−	+	+	−	−	+	−
Lymphoid hyperplasia	−	2	1	−	−	−	2	−	−
Plasmacytosis	4	2–3	−	−	3	3	2	−	3
Tonsil									
Lymphoid depletion	4–5	−	−	5	−	−	−	−	4
Epithelial degeneration/necrosis	4–5	−	−	5	4	1	−	5	4
Epithelial hyperplasia	−	−	−	5	4	1	−	−	−
Hemorrhage	−	−	−	+	−	−	−	+	−
Trachea									
Necrosis	5	−	−	5	5	5	−	3	5
Hemorrhage	−	−	−	+	+	+	−	+	+
Esophagus									
Epithelial degeneration/necrosis	4	−	−	5	4–5	−	−	3–4	−
Epithelial hyperplasia	−	−	−	5	4–5	−	−	3–4	−
Hemorrhage	−	−	−	+	−	−	−	+	−
Colon									
Epithelial degeneration/necrosis	5	−	−	−	2	−	−	3–4	−
Hemorrhage	−	−	−	−	−	−	−	+	+
Nodular necrosis/inflammation	−	−	−	−	−	4	−	−	−

Continued on following page

TABLE 1—*Continued*

Location or type of lesion	Histopathologic score of indicated animal no.[a]								
	1	2	3	4	5	6	7	8	9
Urinary bladder									
Urothelial degeneration/necrosis	2	−	−	−	−	−	N/A	3	1
Epithelial hyperplasia	−	−	−	3	−	−	N/A	−	−
Hemorrhage	−	−	−	+	−	−	N/A	+	−
Femoral bone marrow									
Necrosis	−	−	−	4	−	−	−	3	−
Intravascular fibrin thrombi	−	−	−	+	+	+	−	+	−

[a] Necropsy occurred as follows: monkey no. 1, 12 dpi; no. 2, 25 dpi; no. 3, 25 dpi; no. 4, 12 dpi; no. 5, 16 dpi; no. 6, 22 dpi; no. 7, 21 dpi; no. 8, 8 dpi; no. 9, 8 dpi. 1, minimal; 2, mild; 3, moderate; 4, marked; 5, severe; NA, tissue not collected; −, lesion absent; +, lesion present.

disease had a chance to develop. In an attempt to avoid the production of a lobar pneumonia, a microsprayer with a high pressure syringe attached to the working channel of a standard bronchoscope was evaluated in the second phase of these studies. The inclusion of the microsprayer for delivery of challenge virus allowed for a large-particle aerosol (~8 μm) to be deposited directly above the tracheal carina. Use of the microsprayer reduced the incidence of lobar pneumonia and allowed for production of a clinical disease and pathology that appears to be similar to that produced by an aerosol chamber, albeit with a fraction of the virus. While it is still unclear how closely the disease produced by the microsprayer delivery faithfully mimics human SPOX disease, it clearly has applicability for the evaluation of the risk from aerosol releases of orthopoxviruses in a biological weapons scenario, as well as for the evaluation of candidate therapeutics and vaccines for intervention and/or prevention against this mode of exposure. The increase in the number of cutaneous lesions observed in the microsprayer model as opposed to the classical aerosol model suggests that this model may be more faithful to human disease and further supports the assertion that the microsprayer system is a suitable model system for the study of orthopoxvirus infections. In addition, unlike the aerosol chambers, this system is portable and inexpensive and staff is easily trained in techniques for use. The system requires minimal amounts of virus, and the amount of virus delivered is more controlled than with the aerosol chambers.

In a natural setting the index case in a MPOX or VARV outbreak may very well be through a break in the skin or, for MPOX, through contact with an infected animal. However, human-to-human spread will likely occur by the respiratory route or by close contact. In addition, in the scenario of a purposeful release of MPOX or VARV, an aerosol exposure would be the most likely mode of release. Comparison of NHPs exposed either by the aerosolized virus delivered by bronchoscope or intravenously demonstrated that classic MPOX disease can be achieved with similar challenge doses of virus; however, severe disease can be achieved using intratracheal delivery with a greater range of challenge doses. It is unclear why the normal steep dose-response curve reported for intravenous challenge of MPOX and VARV was not observed for delivery of MPOX intratracheally. Interestingly the intratracheal aerosol delivery did allow for a longer incubation period, more closely mimicking the incubation during human SPOX disease. At the lowest challenge dose (3.42×10^6), clinical onset of disease (oral lesions) did not occur until postinfection day 8, and, at their peak, lesion numbers reached in the hundreds for all three animals. This number of lesions, while lower than what is observed in intravenous exposure, is higher than what has previously been seen with many aerosol challenges. Of interest, lesion counts in human MPOX cases seen in the Democratic Republic of Congo can range from <50 to the thousands. The reason for the tremendous range in the number of lesions is unknown.

There were no major pathological differences between dosage groups in this study. While evaluation of terminal lesions in animals challenged intratracheally suggest that many of the gross and histological changes are similar to intravenous and aerosol challenges, the progression of lesion development can be assessed only with a sequential sampling study. Although involvement of the lungs and the development of pneumonia have been described for the intratracheal, aerosol, and intravenous MPOX models, the distribution of lesions is distinct for each model: aerosolized and i.t. administration of virus causes primary bronchopneumonia, whereas i.v. inoculation causes interstitial pneumonia, with the lungs as a secondary target of infection. The pathology of aerosolized MPOX is characterized by fibrinonecrotic bronchopneumonia with systemic dissemination, and death occurs between days 9 to 17 postexposure (18). A review of data from sequential sampling studies of nonhuman primates challenged intravenously demonstrated that mild or moderate fibrinonecrotic interstitial pneumonia and pleuritis appeared on day 5 following intravenous MPOX exposure. Histologically the interstitium was expanded by inflammatory cells (e.g., monocytes and neutrophils) with foci of necrosis or, in terminally ill animals, more widespread necrosis, fibrin, and inflammation. Immunohistochemical staining of the lungs for viral antigen was typically positive throughout the course of the disease, beginning on day 5 postinfection, and the viral load of monkeypox virus in the lung peaked at PID 8 in the intravenous model. Data from terminal animals on multiple intravenous challenge studies confirm that fibrinonecrotic interstitial pneumonia is a common finding. Although there are differences in lesion distribution, the observation of pneumonia and lung involvement in intratracheal/aerosol and i.v. models further supports the utility of the intratracheal model. However, further studies will be needed to assess whether the pathology associated with intratracheal installation of virus is more severe or progresses more rapidly than either the intravenous or aerosol model. A more in-depth assessment of the

progression of lesions, host responses, and pathophysiologic changes will require a sequential sampling study and a natural history study with assessment of the clinical progression via telemetry devices.

The cause of pneumonia in humans (described in the literature as "bronchopneumonia") is not clear. Some authors attributed it directly to the virus (11), while others believe it was associated with secondary bacterial infections (1, 3). Additionally work is needed to assess the significance of the pathology observed with the lungs, and it will be critical that future works focus on the comparison of NHP data with human data to assess how faithful the intratracheal models reflect human SPOX disease and the potential long-term consequences of the significant lesions in the lungs observed in some animals. This will entail more detailed and focused efforts on the collection of historical human clinical samples as well as the description of the epidemiology of human monkeypox disease.

Although hemorrhagic disease has not been described for natural cases of human MPOX or experimental MPOX infection in NHPs, it has been well characterized for smallpox in humans and for the VARV NHP animal model (8). It appears, however, that several animals in this experiment exhibited a hemorrhagic manifestation of MPOX disease, as intravascular fibrin thrombi and hemorrhage in multiple organs were observed in 1/3 high-dose animals and 2/3 middle-dose animals. Additionally, in our experience utilizing a constant dose of i.v. or i.t. MPXV, we have seen this manifestation in up to 50% of the animals in several studies at our facility. It is unknown whether this manifestation of the disease is caused by an overactive host immune response, pre-existing immunosuppressive condition, virulence of the virus, due to the complex interaction between the host and the virus, or a combination of these factors. Overall, the animals with a hemorrhagic manifestation of disease had more widespread immunoreactivity than animals that did not display hemorrhagic disease. Clinicopathologic parameters (i.e., coagulation profiles and D-dimers) will be important correlates to evaluate in future studies.

In summary, this paper reports the development of a novel MPOX model that could serve as an alternative to classic aerosol challenge models. While more work will be required to characterize the sequential development of disease and pathology, the data presented in this report demonstrate that this model already has potential for the evaluation of risk from aerosol releases or challenges as well as evaluation of vaccine and therapeutic efficacy. In addition, the deaths of 1/3 monkeys challenged with VARV using a bolus dose of virus verifies that NHPs are susceptible to infection with VARV via routes other than intravenous methods. Based on the success of the microsprayer with MPOX in conjunction with the VARV bolus intratracheal challenge experiments, there is sufficient data to suggest that a microsprayer model could be developed for VARV infection. However, there is not sufficient data to suggest that a VARV microsprayer model would allow for a reduction in the challenge dose of virus needed to achieve significant disease. Finally, the difference in the size of particles generated with the microsprayer and collison nebulizer raises the question of whether particle size is important for disease progression and severity. Previous reports using a collison nebulizer suggested that the challenge dose could be reduced to 1×10^4 PFU and still achieve a lethal model. However, fewer cutaneous lesions were noted with this model. Based on the data in the literature as well as the data presented in this report, future studies may be warranted to evaluate whether particle size impacts disease presentation, morbidity, or fatality.

ACKNOWLEDGMENTS

This work was supported by Department of Homeland Security/National Biodefense and Countermeasures Center, Contract number RSRD-05-00378.

The opinions, interpretations, conclusions, and recommendations are those of the authors and are not necessarily endorsed by the U.S. Army.

REFERENCES

1. **Bras, G.** 1952. The morbid anatomy of smallpox. Doc. Med. Geogr. Trop. **4:**303–351.
2. **Centers for Disease Control and Prevention.** 2003. Update: multistate outbreak of monkeypox—Illinois, Indiana, Kansas, Missouri, Ohio, and Wisconsin, 2003. MMWR Morb. Mortal. Wkly. Rep. **52:**642–646.
3. **Councilman, M., G. B. Magrath, and W. R. Brinckerhoff.** 1904. The pathological anatomy and histology of variola. J. Med. Res. **11:**12–135.
4. **Federal Register.** 2002. New drug and biological drug products; evidence needed to demonstrate effectiveness of new drugs when human efficacy studies are not ethical or feasible, final rule. Fed. Regist. **67:**37988–37998.
5. **Fenner, F., W. R., R. Wittek, and K. R. Dumbell.** 1989. The Orthopoxviruses. Academic Press, San Diego, CA.
6. **Huggins, J., et al.** 2009. Nonhuman primates are protected from smallpox virus or monkeypox virus challenges by the antiviral drug ST-246. Antimicrob. Agents Chemother. **53:**2620–2625.
7. **Hutin, Y. J., et al.** 2001. Outbreak of human monkeypox, Democratic Republic of Congo, 1996 to 1997. Emerg. Infect. Dis. **7:**434–438.
8. **Jahrling, P. B., et al.** 2004. Exploring the potential of variola virus infection of cynomolgus macaques as a model for human smallpox. Proc. Natl. Acad. Sci. U. S. A. **101:**15196–15200.
9. **Jordan, R., et al.** 2009. ST-246 antiviral efficacy in a nonhuman primate monkeypox model: determination of the minimal effective dose and human dose justification. Antimicrob. Agents Chemother. **53:**1817–1822.
10. **Kulesh, D. A., et al.** 2004. Smallpox and pan-orthopox virus detection by real-time 3′-minor groove binder TaqMan assays on the Roche LightCycler and the Cepheid Smart Cycler platforms. J. Clin. Microbiol. **42:**601–609.
11. **Lillie, R.** 1930. Smallpox and vaccinia: the pathologic histology. Arch. Pathol. **10:**241–291.
12. **Martin, D. B.** 2002. The cause of death in smallpox: an examination of the pathology record. Mil. Med. **167:**546–551.
13. **Meyer, H., et al.** 2002. Outbreaks of disease suspected of being due to human monkeypox virus infection in the Democratic Republic of Congo in 2001. J. Clin. Microbiol. **40:**2919–2921.
14. **National Research Council.** 1996. Guide for the care and use of laboratory animals. National Academy Press, Washington, DC.
15. **Prophet, E. B., B. Mills, J. B. Arrington, and L. H. Sobin.** 1992. Laboratory methods for histotechnology. Armed Forces Institute of Pathology, Washington, DC.
16. **Rimoin, A. W., et al.** 2007. Endemic human monkeypox, Democratic Republic of Congo, 2001–2004. Emerg. Infect. Dis. **13:**934–937.
17. **Rimoin, A. W., et al.** 2010. Major increase in human monkeypox incidence 30 years after smallpox vaccination campaigns cease in the Democratic Republic of Congo. Proc. Natl. Acad. Sci. U. S. A. **107:**16262–16267.
18. **Zaucha, G. M., P. B. Jahrling, T. W. Geisbert, J. R. Swearengen, and L. Hensley.** 2001. The pathology of experimental aerosolized monkeypox virus infection in cynomolgus monkeys (Macaca fascicularis). Lab Invest. **81:**1581–1600.